PLANNING MALAYSIA:
Journal of the Malaysian Institute of Planners
VOLUME 21 ISSUE 5 (2023), Page 1 – 16

CLIMATE VARIABILITY IN RELATION TO LAND USE AND LAND COVER (LULC) CHANGES IN KOTA BHARU, KELANTAN, MALAYSIA

Balqis Ibrahim[1], Zulfa Hanan Ash'aari[2]

[1,2] *Department of Environment, Faculty of Forestry and Environment,*
UNIVERSITI PUTRA MALAYSIA

Abstract

The process of rapid urbanization has significantly altered natural landscapes and contributed to climate variability. Due to urbanization, land surface characteristics are changing, resulting in a changing thermal climate making cities warmer than surrounding rural areas. The study utilized remote sensing and Geographic Information System (GIS) technologies to analyze the connection between land use and land cover (LULC) change and climatic variability in Kota Bharu, Kelantan, Malaysia. The outcome showed that the greatest LULC change resulted from converting vegetation and bare land into built-up areas, with 25.46% and 10.17% respectively. This represents the rapid expansion of urban land caused by population growth. LST increment averaged 3.65°C in the last decade due to this massive increase in built-up areas. A linear regression analysis between LST and LULC indices, NDBI and NDVI shows that they are positively correlated. By understanding these two variables, land use planning could be further improved, hence, reducing the city's vulnerability towards climate variability.

Keywords: Change detection, Geospatial analysis, Land change, Supervised classification

[2] Senior Lecturer at Universiti Putra Malaysia. Email: zulfa@upm.edu.my

INTRODUCTION

Climate change is widely recognized as one of the most severe issues confronting humankind and nature. It is a driver of the global crisis that affects every facet of our lives and future. The Intergovernmental Panel on Climate Change (IPCC)'s Fifth Assessment reported that the global average surface temperature rose 0.85°C from 1880 to 2012. It is expected to rise from 2.6°C to 4.8°C by the end of the 21st century (2081–2100) compared to the year 1986 to 2005 under high-emission scenarios (IPCC, 2014). Recent studies show that rapid urbanization that takes place in cities drives climate change (How Jin Aik, Ismail, & Muharam, 2020; Ibrahim, 2020; Alzubade, Ozcan, Musaoglu, & Türkeş, 2021). Urbanization has a number of negative effects, one of which is the modification of the thermal climate, which makes cities warmer than their rural surroundings (Rawat, Biswas, & Kumar, 2013).

The rising temperature (Kwan, Tangang, & Juneng, 2013; Moomaw et al., 2018) and an erratic rainfall trend are Malaysia's most visible climate changes (Khan, Shaari, Nahar, Baten, & Nazaruddin, 2014; Md Saad et al., 2023). According to Rahman (2018), Malaysia is estimated to be hotter by 2050, with a temperature increase of up to 1.5°C compared to just 0.6 °C over the past 28 years (World Bank, 2020). The use of satellite Remote Sensing (RS) and Geographical Information System (GIS) technology to analyze LULC transitions and hydrology purposes has been widely accepted (Khan et al., 2014; Latif & Kamsan, 2018; Zhou, Zhang, & Guo, 2019). As a result, analyzing the spatio-temporal changes in LULC has become one of the most important research topics in recent decades (Khan et al., 2014).

This study is intended to focus on whether there is valid evidence on climate variability in association with LULC alteration in the study area. The outcome of this study is expected to be essential for effective land use management and sustainable urban planning of the area, bringing awareness to the authorities and residents to make wiser decisions on land use.

RESEARCH METHODOLOGY

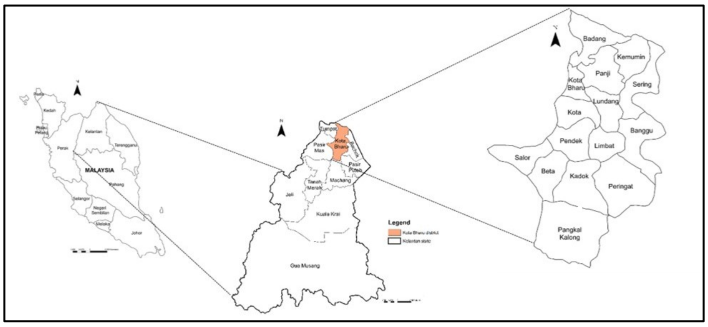

Figure 1: Geographical location of Kota Bharu district in Malaysia

Located on the east coast of peninsular Malaysia, Kelantan has a total area of approximately 15,100 km^2. The study area of Kota Bharu (Figure 1) is the capital city and major urban centre of the state that is in the northern part of Kelantan where the state's commercial and administrative hub is located. It has a typical tropical climate pattern, with an annual precipitation of 2500 mm and a mean temperature of 27.5 ºC (Tan, Ibrahim, Yusop, Chua, & Chan, 2017). Having a high-temperature increase (Ibrahim, 2020), the city is becoming increasingly vulnerable to natural disasters and temperature shifts due to its geographical characteristics, unplanned urbanization, and proximity to the sea (Faizalhakim et al., 2017).

Data Acquisition

This research is conducted using the satellite images of Kota Bharu from the year 1990 until 2020 which were obtained from the official website of the United States Geological Survey (USGS) https://earthexplorer.usgs.gov. The data were derived from Landsat 5 TM, Landsat 7 ETM+, and Landsat 8. Due to its availability and extensive coverage (How Jin Aik, Ismail, & Muharam, 2020), the Landsat imagery was chosen. The date of data that was taken was chosen based on the availability of data throughout the study year and region. Prior to the analysis, the satellite data were further screened for minimum cloud or haze coverage. As for climate variability, LST, which is estimated from the thermal emissivity of land surfaces contained in remote sensing images, was used in this research to represent temperature. The LST is an excellent indicator of long-wave and incoming solar irradiance, which impacts all LULC classes (Alzubade, Ozcan, Musaoglu, & Türkeş, 2021).

Data Processing & Analysis

Image Classification & LULC change mapping

Satellite images extracted from Landsat 5 TM, Landsat 7 ETM+, and Landsat 8 were used for LULC classification. The supervised image classification and change detection were applied using remote sensing software. The use of remote sensing data for change detection was based on the understanding that changes in land cover result in changes in radiance values, which may be remotely measured (Jin Aik et al., 2020). The land use for each year was reclassified into several major land uses which are the bare land, vegetation area, urban area, and water bodies. To ensure the land cover was correctly assigned, Google Earth images were used as a cross-reference. The classification of LULC was mapped using ArcGIS 10.8 to observe and visualize the change. The multiple LULC classes of the research area were represented using the stratified random approach for the accuracy evaluation. The accuracy was evaluated using 100 pixels per category based on visual interpretation and ground truth data. The non-parametric Kappa test was also used to gauge the degree of categorization accuracy.

Land Surface Temperature

In this study, the LST value will be extracted through pixel-based calculation. The value of each pixel is calculated using 1:

$$Land\ Surface\ Temperature\ (°C) = (pixel\ value \times 0.02) - 273.15 \quad (1)$$

From 1990 to 2020, the mean value is determined by comparing the 30 years of monthly images. The monthly mean LST is then measured using a formula by Patel, Joshi, & Bhatt (2017) in which the number of 8-day images in each of a given month is divided by all non-zero occurrences in that month.

NDBI and NDVI Calculation

This index detects urban areas with higher reflectance in the shortwave-infrared (SWIR) region than in the near-infrared (NIR) region for NDBI. It is calculated by dividing the SWIR by the NIR (Equation (2)). The NDBI was originally developed to work with Landsat TM bands 5 and 4 (Zha, Gao, and Ni, 2003). It will, however, function with any multispectral sensor having a SWIR band of 1.55-1.75 µm and an NIR band of 0.76-0.9 µm.

$$NDBI = (SWIR - NIR)/(SWIR + NIR) \quad (2)$$

NDVI is calculated using two bands with high reflectance in the NIR spectrum and strong absorption in the red wavelength as shown in Equation (3) (Xue & Su, 2017). The NDVI scale runs from 1 to -1. The greatest NDVI value implies healthy vegetation, whereas the lowest NDVI value indicates a lack of vegetation (Osunmadewa, Gebrehiwot, Csaplovics, & Adeofun, 2018). Near-infrared wavelengths of the electromagnetic spectrum are used to calculate the NDVI, along with the red bands of the visible spectrum, which was proposed by Rouse (1974). It is calculated using an equation where NIR stands for near-infrared reflection, while RED stands for red reflection (Gessesse & Melesse, 2019). NIR and RED are the reflectance emitted by the satellite MSS Landsat 5 in the NIR band 7 and visible red band 5, respectively. The NIR band for TM and ETM+ sensors would be band 4, and the RED band is band 3. Lastly, with the OLI sensor, band 5 and band 4 are the NIR and RED bands, respectively (Aslanov et al., 2021). As a result, the following formula yields the NDVI:

$$NDVI = (NIR - RED)/(NIR + RED) \quad (3)$$

Climate variability

To define the climate variability of the study area, the temporal trend of the data was observed and analysed using the Man Kendall and Sen's Slope Estimator. The Man Kendall test is widely used to detect meteorological variable patterns (Saimi, Hamzah, Toriman, Jaafar, & Tajudin, 2020). It is a nonparametric test that can be used to find monotonic trends in a series of climate data (Mudelsee, 2019). Monthly and annual trend analyses were conducted to detect any significant climate patterns from the year 1990 until 2020. The Mann Kendall trend analysis generates three outputs that decide whether a trend occurs. A positive z-statistic value indicates an upward trend, while a negative z-statistic value indicates a downward trend. The pattern is considered significant if the p-value is less than 0.05 (95% confidence level) (Kamal, Ashaari, & Abdullah, 2019). Sen's Slope and ArcGIS 10.8 were used to know the magnitude of the trend per year and map the LST of the study area respectively.

The relationship between LULC and climate variability

In order to determine the relationship between LULC and climate variability, a linear correlation coefficient analysis was used. This analysis served to unveil the connection between LULC and climate variability. The determination of whether the relationship is positively or negatively correlated was based on the R^2 values.

RESULTS AND DISCUSSION

Land Use and Land Cover (LULC)

Table 1 summarizes the trend of LULC from 2000 to 2020 based on the four classes that are extracted from the Kota Bharu study area. When the study began initially in the year 1990, the percentage of the total study area was dominated by vegetation, covering 64.22% of the total study area, followed by bare land

(21.44%), built-up area (11.69%) and water bodies (2.39%). The trend was observed for all LULC classes from the year 1990 until 2020. Throughout the 30 years, the built-up area had been the most increased area, from 11.96% to 32.24%, totaling a total of 20.28% increment. The percentage of vegetation had also decreased from 64.22% to 49.92%, making up a total of 14.30% for 30 years. This is followed by bare land, which had been decreasing from 21.44% to 15.84%. In 30 years, the total area had decreased by 5.60%. Meanwhile, the water bodies have not been decreasing at the same rate as bare land or vegetation, but it still has a slight decrease of 0.35%.

Table 1: Area of the LULC classification for 1990, 2000, 2010, and 2020 map

	1990		**2000**		**2010**		**2020**	
	Area (km^2)	**%**	**Area (km^2)**	**%**	**Area (km^2)**	**%**	**Area (km^2)**	**%**
Built-up Area	48.37	11.96	104.02	25.73	105.97	26.21	130.33	32.24
Vegetation	259.64	64.22	250.72	62.01	244.86	60.56	201.85	49.92
Water Bodies	9.62	2.38	9.55	2.36	8.63	2.13	8.09	2.00
Bare land	86.69	21.44	40.02	9.90	44.86	11.10	64.05	15.84

Accuracy Assessment

The overall classification accuracy and kappa coefficient obtained for the LULC classification accuracy evaluation of the 1990, 2000, 2010, and 2020 data were used to measure the classification quality. As a whole, LULC categorization scores varied from 93% to 97.5% across the four years, The agreement index of Kappa ranged from 0.88 to 0.96 (Table 2). For the study region, these Kappa values for the four categorization findings are acceptable since they meet Anderson's (1976) classification scheme's minimal accuracy requirement of 85%.

Table 2: Accuracy assessment of the LULC classification in Kota Bharu, Kelantan

	1990	**2000**	**2010**	**2020**
Overall	95.00	93.75	96.25	97.50
Kappa	0.93	0.88	0.95	0.96

Land Use and Land Cover (LULC) Changes

For the period of 1990 to 2000 (Figure 2(a)), the LULC change patterns reveal that the vegetation area was converted into a built-up area that summed up to a total of 13.78%, followed by bare land to vegetation with 13.19%. Meanwhile, from 2000 to 2010 (Figure 2(b)), the greatest LULC change was for a built-up area to vegetation, with 10.12%. This may be due to the expansion of the paddy field in the area (Mahamud et al., 2019). It was closely followed by vegetation to built-up area and bare land conversions, with 9.82% and 8.44%, respectively. From 2010 to 2020 (Figure 2(c)), the largest percentage of LULC change can be seen as a result of vegetation conversion into a built-up area and bare land, with 33.23% and 21.18%, respectively, contributing to the highest percentage of LULC change over the years (Table 3).

Based on a LULC modelling study by Mahamud et al. (2019) in Kelantan, it is believed that Kelantan has undergone major changes in the past few decades such as the incrementing of built-up areas and a reduction in forest areas. The built-up areas are mainly in the northern part of the state, i.e., Kota Bharu has been expanding at a steady rate, and there has also been an increase of urban sprawl within the city. According to the simulated LULC 2025, sprawl development is also taking place, which should prompt local planners to map out the development in Kelantan, especially in the Kota Bharu area.

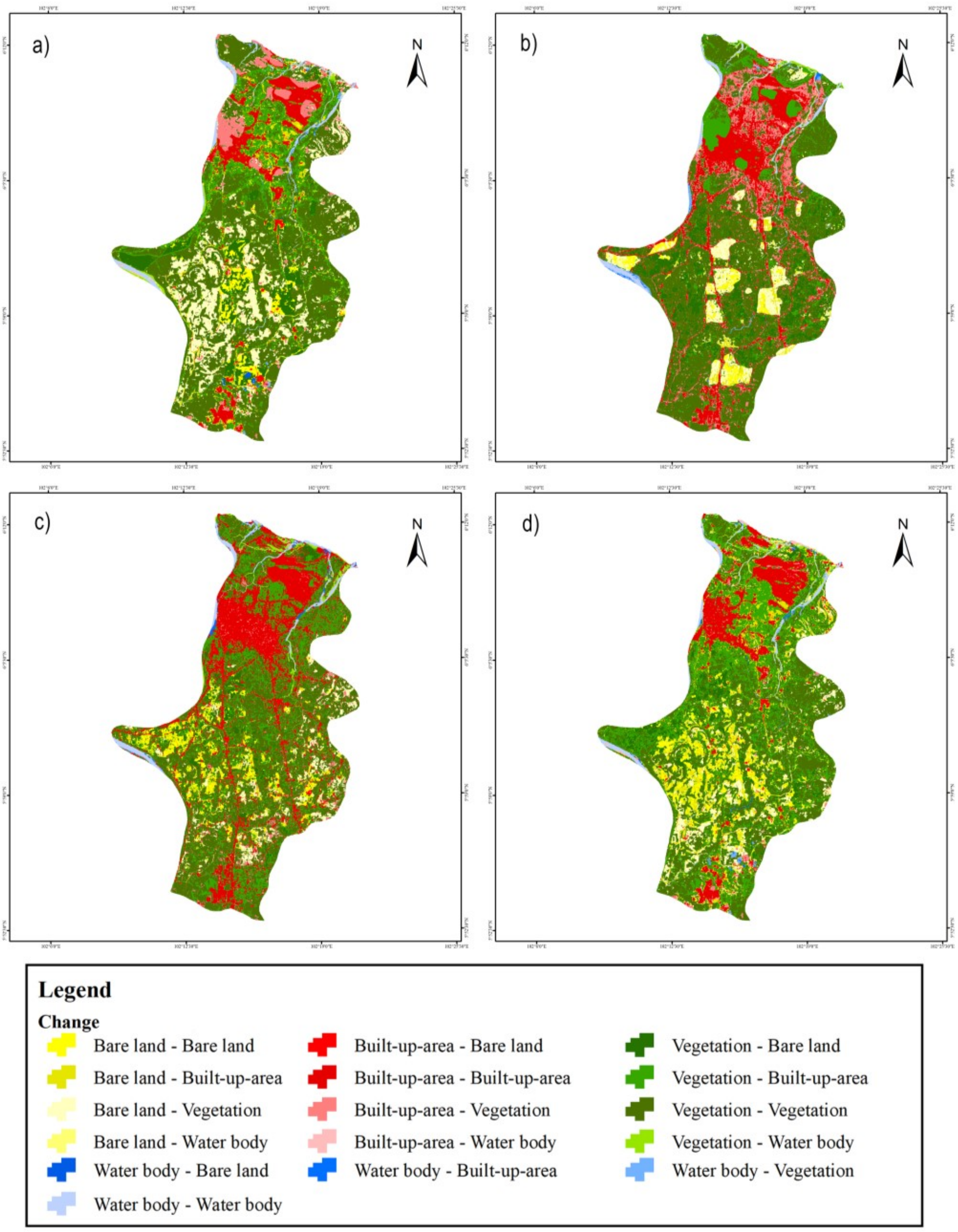

Figure 2: LULC Change Maps of Kota Bharu a) 1990-2000 b) 2000-2010 c) 2010-2020 d) 1990-2020

Table 3: LULC change area and percentage of Kota Bharu for the year 1990-2020

	1990-2000		**2000-2010**		**2010-2020**		**1990-2020**	
	Area (km^2)	**%**	**Area (km^2)**	**%**	**Area (km^2)**	**%**	**Area (km^2)**	**%**
Built-up area	28.10	6.96	59.56	14.74	84.58	20.93	40.91	10.13
Built-up area to Vegetation	17.95	4.44	40.88	10.12	13.33	3.30	4.51	1.12
Built-up area to Bare land	1.92	0.47	2.19	0.54	8.14	2.01	2.05	0.51
Built-up area to Water bodies	0.38	0.09	0.76	0.19	0.79	0.20	0.89	0.22
Vegetation	178.88	44.28	175.96	43.55	134.25	33.23	132.64	32.83
Vegetation to Built-up area	55.68	13.78	39.69	9.82	85.58	21.18	102.85	25.46
Vegetation to Bare land	24.88	6.16	34.08	8.44	19.99	4.95	22.59	5.59
Vegetation to Water bodies	1.98	0.49	1.80	0.45	4.25	1.05	3.30	0.82
Bare land	11.85	2.93	7.69	1.90	13.13	3.25	16.21	4.01
Bare land to Built-up area	19.07	4.72	6.88	1.71	14.36	3.55	41.06	10.16
Bare land to Vegetation	53.30	13.19	24.67	6.11	16.68	4.13	26.41	6.54
Bare land to Water bodies	0.52	0.13	0.38	0.09	0.13	0.03	1.06	0.26
Water bodies	6.61	1.64	5.90	1.46	6.59	1.63	6.47	1.60
Water bodies to Built-up area	0.53	0.13	0.69	0.17	1.42	0.35	1.10	0.27
Water bodies to Vegetation	1.42	0.35	2.56	0.63	0.76	0.19	1.47	0.36
Water bodies to Bare land	0.98	0.24	0.34	0.08	0.08	0.02	0.49	0.12

Normalized Difference Built-up Index (NDBI)

The NDBI density classes are inversely related to the green index. Higher values of NDBI are seen to be clustered around the built-up and bare land area (Figure 3). The NDBI values of each LULC class for each year are shown in Table 4.

Table 4: NDBI values of Kota Bharu in the years 1990, 2000, 2010, and 2020

	1990	**2000**	**2010**	**2020**
Waterbodies	-0.5897 - -0.2186	-0.6363 - -0.3171	-0.9285 - -0.2744	-0.5155 - -0.3253
Vegetation	-0.2186 - -0.0248	-0.3171 - -0.0566	-0.2744 - -0.0814	-0.3253- -0.2560
Bare land	-0.0248 - 0.1274	-0.0566 - 0.0645	-0.0816 - 0.1227	-0.2560 - -0.0937
Built-up area	0.1274 - 0.5789	0.0645 - 0.7142	0.1227 - 0.5774	0.1937 - 0.3380

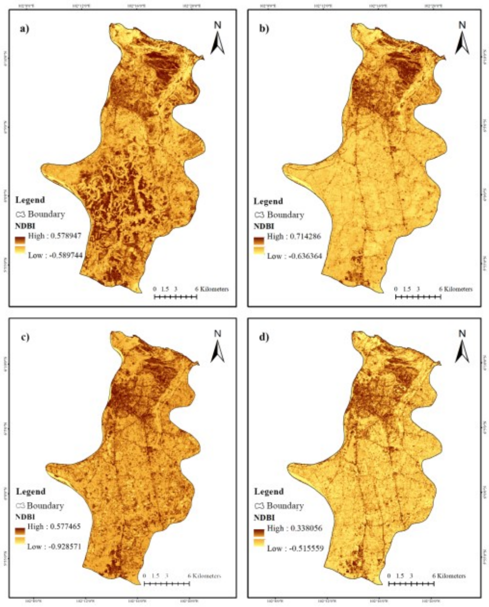

Figure 3: NDBI maps of a) 1990 b) 2000 c) 2010 and d) 2020 in Kota Bharu

Normalized Difference Vegetation Index (NDVI)

The expansion of lower NDVI values depicts the decrement of the vegetation area from 1990 to 2020 (Figure 4). The NDVI values ranged from 0.3498 - 0.7222 to 0.1773 - 0.4218. The waterbody has ranged from -0.4893 - -0.0474 in the year 1990 and ranged from -0.3331 - 0.0481 in the year 2020. Table 5 inputs the detailed NDVI values of each LULC class.

Table 5: NDVI values of Kota Bharu in the years 1990, 2000, 2010, and 2020

	1990	2000	2010	2020
Waterbodies	-0.4893 - -0.0474	-0.6999 - -0.0893	-0.7062 - -0.3562	-0.3331 - 0.0481
Vegetation	-0.0474 - 0.2541	-0.0893 - 0.3137	-0.3562 - -0.0964	0.0481 - 0.2501
Bare land	0.2541 - 0.3498	0.3137 - 0.5271	-0.0964 - 0.1451	0.2501 - 0.3773
Built-up area	0.3498 - 0.7222	0.5271 - 0.8117	0.1451 - 0.5838	0.1773 - 0.4218

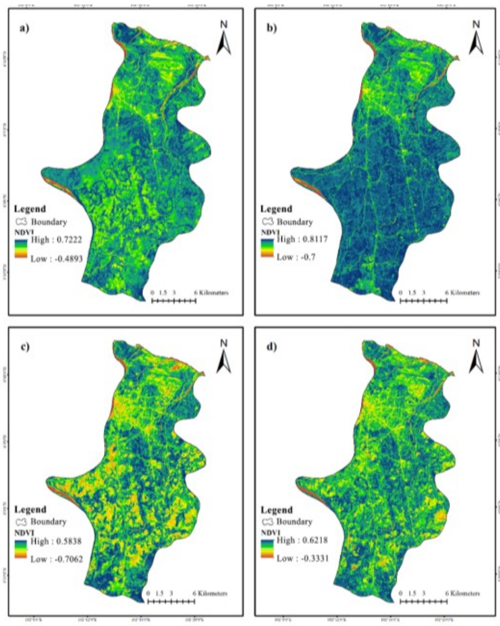

Figure 4: NDVI maps of a) 1990 b) 2000 c) 2010 and d) 2020 in Kota Bharu

Land Surface Temperature (LST)

Figure 5 illustrates the LST distribution in Kota Bharu. Throughout the 30 years, the maximum LST had decreased from 34.86°C to 29.19°C from 1990 to 2000, but continued to rise from 2000 until 2020, with the highest in 2020 at 35.70°C. The lowest minimum LST was 16.56°C in 1990. Over the last twenty years, the average LST has increased steadily from 22.62°C to 26.27°C, which is a 3.65°C rise. The highest LST values range near the city's urban area. As humans are heat carriers and contribute to the anthropogenic heat dispersion of the surrounding region, their presence in these locations has a substantial effect on the total LST. Known as thermal convection, this occurs when the heat rises while the cold air falls, and under massed settings, this heat is likely to attach to surrounding surfaces, such as those of buildings (Jin Aik et al., 2020). High NDBI values also indicate higher LST values and vice versa for the NDVI. Table 6 displays detailed temperatures of the study area.

Table 6: Average LST of Kota Bharu in the years 1990, 2000, 2010, and 2020

	1990	2000	2010	2020
Maximum (°C)	34.86	29.19	34.86	32.70
Minimum (°C)	16.56	17.33	18.38	20.17
Average (°C)	26.47	22.62	25.60	26.27
Maximum (°C)	34.86	29.19	34.86	32.70

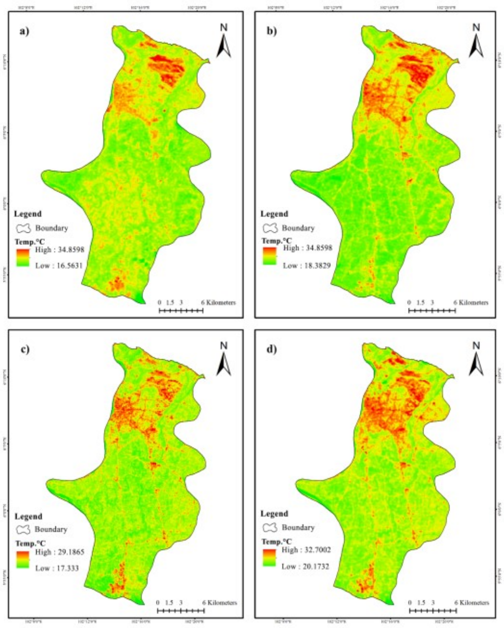

Figure 5: LST maps of a) 1990 b) 2000 c) 2010 and d) 2020 in Kota Bharu

Trend Analysis

The Mann-Kendall trend test analysis indicated the annual trend of LST in Kota Bharu. The Mann-Kendall test generates a positive result for the z-statistic. Based on the positive value, this implies that there is a strong increasing trend of the LST from 1990 to 2020. With a p-value of 0.0382, indicating that the result is statistically significant. Sen's Slope of 0.049 denotes the magnitude of the trend each year. In this scenario, the average annual increase is found to be 0.049°C per year (Table 7).

Table 7: Annual trend of Kota Bharu

	Z-statistic	P-value	Sen's Slope
Annual	1.0190	0.0382*	0.049

*Indicate statistically significant result

LULC change and LST relationship

To study the relation between the LULC indices and land surface temperature, 200 randomly selected sample points from LST, together with NDBI and NDVI data were applied to fit the regression and determine the Pearson correlation coefficients. The R^2 values provide insights into the strength and nature of the relationship between NDVI and LST, NDBI and LST for each respective year.

A regression analysis was performed for the years 1990, 2000, 2010, and 2020 between the LST and both LULC indices; NDBI and NDVI. For LST and NDBI, it reveals R^2 values of 0.4374, 0.6323, 0.5378, and 0.4994 for 1990, 2000, 2010, and 2020, respectively. Positive values show that the LST value rises in tandem with the NDBI values (Figure 6). The results indicate that the link between NDBI (urbanization or built-up areas) and LST suggests that as urbanization increases in an area, there is also a notable tendency for the land surface temperature to rise.

The NDVI-LST graph also showed a positive relationship. A regression analysis performed for the years 1990, 2000, 2010, and 2020 between the LST and the LULC index; the NDVI, reveals R^2 values of 0.3189, 0.3551, 0.1919, and 0.1428 respectively (Figure 7). This also suggests that there is a bidirectional relationship between them just as the NDBI-LST. LST can impact the phenology of vegetation and consequently, NDVI value. Conversely, variations in NDVI (vegetation changes) could also change LST such as a decrease in vegetation cover might lead to higher temperatures due to reduced shading and cooling effects of vegetation.

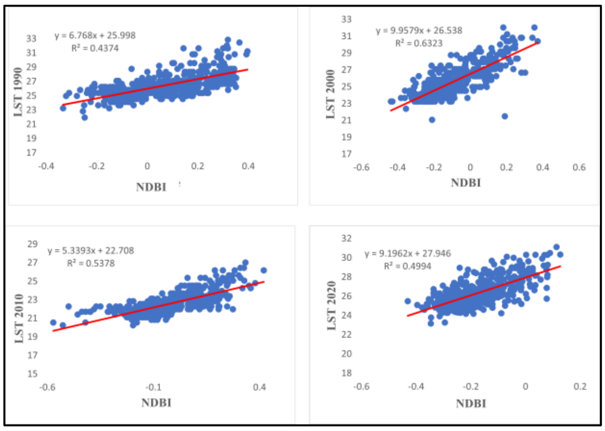

Figure 6: Regression analysis between NDBI and LST in Kota Bharu

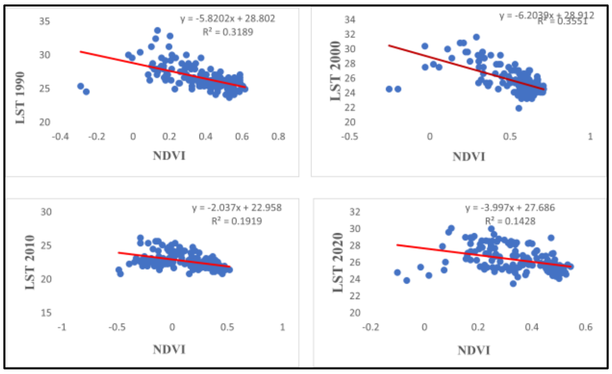

Figure 7: Regression analysis between NDVI and LST in Kota Bharu

CONCLUSION

A low-cost change analysis based on remote sensing data was conducted in Kota Bharu, Kelantan, to quantify and map the changing patterns of LULC using remote sensing data. The analysis and mapping of LULC in Kota Bharu laid the groundwork for strategic planning, management, and decision-making. However, multispectral satellite imagery with very high resolution would allow for more accurate details about the changes in the area.

According to the findings, most LULCs were converted into built-up areas between 1990 and 2020. The expansion of urban land is a result of vast population growth, as evidenced by the expansion of urban land in Kota Bharu. This region is a popular place to live because it is connected to other desirable cities such as Bachok, Tumpat, and Pasir Mas. During the observed period, there was also a 14.30% loss of vegetation and a 5.60% decrease in bare land for future development. The relationship between LULC and LST can be emphasized as how surfaces with high albedo and low absorptivity reflect heat, contributing to regional climate variability. A p-value of 0.0382 from the trend analysis for LST indicates that the result is statistically significant with an average annual increase of 0.049°C per year. The regression analysis results between the LULC indices and the associated LST values support this claim. In general, the increase in temperature in Kota Bharu is found to be affected by changes in LULC, with a positive correlation between the LULC indices, NDBI and NDVI with LST. As a result, proper land management is required to reduce the city's vulnerability to climate variability. Although many more indices are available, only the specified LULC indices have been used in this study. The influencing elements that may alter LST in urban settings, such as building height, density, and material, as well as seasonal changes, have not been included as they are difficult to detect in spatial datasets.

REFERENCES

Alzubade, M., Ozcan, O., Musaoglu, N., & Türkeş, M. (2021). Observed impacts of climate variability on LULC in the Mesopotamia region. *Computers, Materials & Continua*, *67*(2), 2255–2269. doi:10.32604/cmc.2021.013565

Anderson, J. R., Hardy, E. E., Roach, J. T., & Witmer, R. E. (1976). A land use and land cover classification system for use with remote sensor data. *Professional Paper*. doi:10.3133/pp964.

Aslanov, I., Mukhtorov, U., Mahsudov, R., Makhmudova, U., Alimova, S., Djurayeva, L., & Ibragimov, O. (2021). Applying remote sensing techniques to monitor green areas in Tashkent Uzbekistan. *E3S Web of Conferences*, *258*, 04012. doi:10.1051/e3sconf/202125804012.

Faizalhakim, A. S., Nurhidayu, S., Norizah, K., Shamsuddin, I., Hakeem, K. R., & Adnan, I. (2017). Climate variability in relation with land use changes over a 30-year period in Kelantan River Basin. *Malaysian Forester*, *80*(1), 12–30.

Gessesse, A. A., & Melesse, A. M. (2019). Temporal relationships between time series CHIRPS-rainfall estimation and eMODIS-NDVI satellite images in Amhara Region, Ethiopia. In A. M. Melesse, W. Abtew, & G. Senay (Eds.), *Extreme Hydrology and Climate Variability* (pp. 81–92). Elsevier.

How Jin Aik, D., Ismail, M. H., & Muharam, F. M. (2020). Land use/land cover changes and the relationship with land surface temperature using Landsat and MODIS imageries in Cameron Highlands, Malaysia. *Land*, *9*(10), 372. doi:10.3390/land9100372.

Ibrahim, M. H. (2020). Impact of urbanization on the formation of urban heat island in Kota Bharu, Kelantan. *Journal of Mechanics of Continua and Mathematical Sciences*, *spl9*(1). doi: 10.26782/jmcms.spl.9/2020.09.00007.

Intergovernmental Panel on Climate Change. (2014). *Climate change 2013 - The Physical Science Basis: Working Group I Contribution To The Fifth Assessment Report Of The Intergovernmental Panel On Climate Change* (Intergovernmental Panel on Climate Change, Ed.). Cambridge, England: Cambridge University Press.

Kamal, N. I. A., Ashaari, Z. H., & Abdullah, A. M. (2019). Spatio-temporal Variability of Heat Exposure in Peninsular Malaysia using Land Surface Temperature. *Disaster Advances*, *12*(12), 1–9.

Khan, M. M. A., Shaari, N., Nahar, A., Baten, M. A., & Nazaruddin, D. A. (2014). *Flood impact assessment in Kota Bharu, Malaysia: A statistical analysis*.

Kwan, M. S., Tangang, F. T., & Juneng, L. (2013). Projected Changes of Future Climate Extremes in Malaysia. *Sains Malaysiana*, *42*(8), 1051–1058.

Latif, Z. A., & Kamsan, M. E. S. (2018). Assessing the relationship of land use land cover on surface temperature in city of Shah Alam, Malaysia using landsat-8 oli. *Revue Des Sciences Fondamentales et Appliquees*, *9*(5S), 514. doi:10.4314/jfas.v9i5s.36

Mahamud, M. A., Samat, N., Tan, M. L., Chan, N. W., & Tew, Y. L. (2019). Prediction of future land use land cover changes of Kelantan, Malaysia. *ISPRS - International Archives of the Photogrammetry Remote Sensing and Spatial Information Sciences*, *XLII-4/W16*, 379–384. doi:10.5194/isprs-archives-xlii-4-w16-379-2019

Md Saad, M. H., Kamarudin, M. K. A., Toriman, M. E., Abd Wahab, N., Ata, F. M., Abu Samah, M. A., … Manoktong, S. N. (2023). Analysis of the flash flood event and rainfall distribution pattern on Relau River basin development, Penang, Malaysia. *PLANNING MALAYSIA JOURNAL*, *21*. doi:10.21837/pm.v21i25.1224

Moomaw, W. R., Chmura, G. L., Davies, G. T., Finlayson, C. M., Middleton, B. A., Natali, S. M., … Sutton-Grier, A. E. (2018). Wetlands in a changing climate: Science, policy and management. *Wetlands (Wilmington, N.C.)*, *38*(2), 183–205. doi:10.1007/s13157-018-1023-8

Mudelsee, M. (2019). Trend analysis of climate time series: A review of methods. *Earth-Science Reviews*, *190*, 310–322. doi:10.1016/j.earscirev.2018.12.005

Osunmadewa, B. A., Gebrehiwot, W. Z., Csaplovics, E., & Adeofun, O. C. (2018). Spatio-temporal monitoring of vegetation phenology in the dry sub-humid region of Nigeria using time series of AVHRR NDVI and TAMSAT datasets. *Open Geosciences*, *10*(1), 1–11. doi:10.1515/geo-2018-0001

Patel, S., Joshi, J. P., & Bhatt, B. (2017). An assessment of spatio-temporal
variability of land surface temperature using MODIS data: A study of
Gujarat state, India. Geography Compass, 11(4), e12312. doi:10.1111/gec3.12312

Rahman, H. A. (2018). Climate change scenarios in Malaysia: Engaging the public. *International Journal of Malay-Nusantara Studies*, *1*(2), 55–77.

Rawat, J. S., Biswas, V., & Kumar, M. (2013). Changes in land use/cover using geospatial techniques: A case study of Ramnagar town area, district Nainital, Uttarakhand, India. *Egyptian Journal of Remote Sensing and Space Sciences*, *16*(1), 111–117. doi:10.1016/j.ejrs.2013.04.002

Rouse, J. W., Jr, Haas, R. H., Schell, J. A., & Deering, D. W. (1974). *Monitoring vegetation systems in the Great Plains with ERTS.*

Saimi, F. M., Hamzah, F. M., Toriman, M. E., Jaafar, O., & Tajudin, H. (2020). Trend and linearity analysis of meteorological parameters in Peninsular Malaysia. *Sustainability*, *12*(22), 9533. doi:10.3390/su12229533

Tan, M. L., Ibrahim, A. L., Yusop, Z., Chua, V. P., & Chan, N. W. (2017). Climate change impacts under CMIP5 RCP scenarios on water resources of the Kelantan River Basin, Malaysia. *Atmospheric Research*, *189*, 1–10. doi:10.1016/j.atmosres.2017.01.008

Wan Ibrahim, W. Y., & Muhamad Ludin, A. N. (2016). Spatiotemporal land use and land cover change in major river basins in comprehensive development area. *PLANNING MALAYSIA JOURNAL*, (4). doi:10.21837/pm.v14i4.160

World Bank. (2020). *Turn Down the Heat: Why a 4°C Warmer World Must Be Avoided*. Washington, DC: Potsdam Institute for Climate Impact Research and Climate Analytics.

Xue, J., & Su, B. (2017). Significant remote sensing vegetation indices: A review of developments and applications. *Journal of Sensors*, *2017*, 1–17. doi:10.1155/2017/1353691

Zha, Y., Gao, J., & Ni, S. (2003). Use of normalized difference built-up index in automatically mapping urban areas from TM imagery. *International Journal of Remote Sensing*, *24*(3), 583–594. doi:10.1080/01431160304987

Zhou, S., Zhang, W., & Guo, Y. (2019). Impacts of climate and land-use changes on the hydrological processes in the Amur River Basin. *Water*, *12*(1), 76. doi:10.3390/w12010076

Received: 26th June 2023. Accepted: 15th August 2023